DRUG ELUTING NANOELECTRODE ARRAY

A Thesis
Presented to
The Academic Faculty

by

Brandon Mattix

In Partial Fulfillment
of the Requirements for the Degree
B. S. Biomedical Engineering with Research Option in Biomedical Engineering
in the
School of Biomedical Engineering

Georgia Institute of Technology
August 2010

DRUG ELUTING NANOELECTRODE ARRAY

Approved by:

Dr. W. Jud Ready, Advisor
School of Materials Science & Engineering
Georgia Institute of Technology

Dr. David W. Stollberg
Georgia Tech Research Institute
Georgia Institute of Technology

Dr. Paul J. Benkeser
School of Biomedical Engineering
Georgia Institute of Technology

Date Approved: 5 August 2010

ACKNOWLEDGEMENTS

This project and progress through the semester would not have been accomplished without the guidance, support, and aid of Dr. Jud Ready. Special thanks to all Georgia Tech Research Institute and Undergraduate Research Opportunities Program staff for seeing potential in this project and awarding me the President's Undergraduate Research Award for the Spring 2010 semester. Additionally, I would like to thank Stephan Turano for helping to create and analyze all results. Also, thanks to George Evagoras for his continued help throughout the project.

TABLE OF CONTENTS

LIST OF FIGURES

LIST OF SYMBOLS AND ABBREVIATIONS

CNT	Carbon Nanotube
VACNT	Vertically Aligned Carbon Nanotube
SEM	Scanning Electron Microscopy
CVD	Chemical Vapor Deposition
PECVD	Plasma Enhanced Chemical Vapor Deposition
ICP	Inductively Couple Plasma
μm	micrometer ($1x10^{-6}$ m)

SUMMARY

In drug delivery, microneedles offer many unique characteristics which can improve the delivery of drugs into delicate tissues and tissue systems. These needles can be fabricated from a variety of materials including metals, ceramics, and polymers. This project aims to demonstrate a carbon nanotube based microneedle is also possible. By growing vertically aligned carbon nanotubes around a pore, these new microneedles can significantly decrease the diameter of needles used for drug delivery into delicate tissue. Needle diameter is an important factor for drug delivery into delicate tissues such as the central nervous system due to the body's natural healing reponse, glial scarring. By significantly decreasing the needle size from millimeters to nanometers, the amount and size of glial scarring can be reduced and therefore improve drug delivery. Although no complete samples were successfully fabricated in this study, much knowledge and insight was gained on the process for CNT-based microneedle fabrication.

CHAPTER 1
INTRODUCTION AND LITERATURE REVIEW

In the medical field, new and more efficient methods of treatment are in high demand. A recent boom in the nanotechnology field has opened a limitless field for expansion and development. Carbon nanotubes (CNTs), in particular, offer unique properties that could revolutionize certain medical procedures. In the area of drug delivery, large needles are currently used to inject solutions into the body. Certain aspects of current hypodermic injections, such as post-injection scarring and poor bolus injection absorption, are effective and have been used and accepted in the medical field for decades. Currently, the smallest needles commercially available have a 300 μm outer diameter.[1] The idea of using a syringe with a 20-100 μm diameter could help significantly improve drug delivery effectiveness and reduce discomfort. One of the main areas which could be affected by this would be drug delivery into the central nervous system and other delicate tissues (i.e, the eye or brain). In these areas, current methods of drug delivery leave glial scars which pose a problem in tissue and central nervous system regeneration.

This project will aim to fabricate needle-quality CNT arrays. Microneedles have been fabricated from other various materials but a CNT based microneedle has not yet been designed. Through multiple trials, a detailed process will be designed for successful fabrication of CNT microneedles. The focus of this project is to demonstrate that these CNT needles can be successfully fabricated.

Carbon Nanotubes

Carbon nanotubes (CNTs) in general are allotropes of carbon.[2] There are two types of CNTs: single-walled CNTs (SWCNTs) and multi-walled CNTs (MWCNTs) (Figure 1). They are grown as graphene sheets in a hollow cylinder shape, with diameters as small as 0.2 nm and lengths as long as 4 cm.[3] CNTs have been found to exhibit length-to-diameter ratios up to 28,000,000:1, a ratio higher than any other material. SWCNTs are composed of one cylinder, while MWCNTs contain multiple cylinders grown around each other. Mechanically, CNTs have been found to be one of the strongest known materials due to their binding properties and interactions with surrounding CNTs.[4] With an axial Young's modulus of 1 TPa, CNTs have been found to

be one of the stiffest materials known. Combined with their capacity to elastically deform under compression,[5] CNTs possess the potential to successfully penetrate tissue surfaces. These properties help assert the notion that the proposed nanosyringes will be able to tolerate forces associated with insertion, intact removal, and normal human movements.

When grown as MWCNTs, an array of nanotubes align themselves into "ropes" that are held together by Van der Waals forces (Figure 2). SWCNTs and MWCNTs exhibit high electrical and thermal conductivity, along with excellent chemical and thermal stability.[2] Certain properties of CNTs are determined by their crystallographic orientations described as: armchair, zigzag, and chiral. In terms of electrical conductivity, armchair CNTs are known to be metallic and therefore good conductors. In zigzag or chiral structures, they are found to be moderate to strong semiconductors with varying band gap lengths.

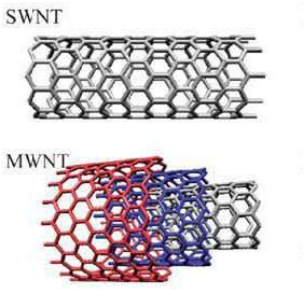

Figure 1: Single-walled vs. Multi-walled CNTs[5]

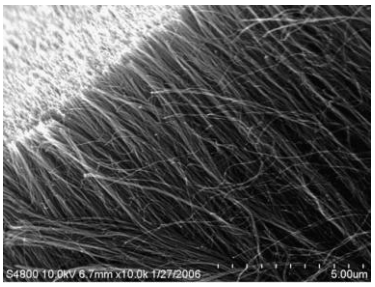

Figure 2: An array of Vertically Aligned CNTs[6]

Glial Scarring

A potential advantage of using the proposed nanosyringe in drug delivery is the capability of avoiding glial scarring. Glial scarring is a natural response from the central nervous system to repair damaged tissue. Due to the low regenerative capacity of the central nervous system, a drug delivery system which could prevent glial scarring is desired.[11] This response serves well in immediately protecting the damaged tissue, but ultimately inhibits axonal regeneration and remyelination.[12] Taking advantage of a nanometer-diameter nanosyringe, a complete lack of gliotic response can be achieved.

With no gliotic response, there would be no damage to the central nervous system or surrounding tissue.

It is unlikely than an entire lack of gliotic response will be seen. However, by decreasing the diameter of tissue penetration, the size of the response could be minimized. Current needles used for drug delivery range in diameter from 3.404 mm to 0.203 mm.[13] Therefore, using CNTs to create a syringe on the μm-level, the diameter of the needle will be decreased by many magnitudes.

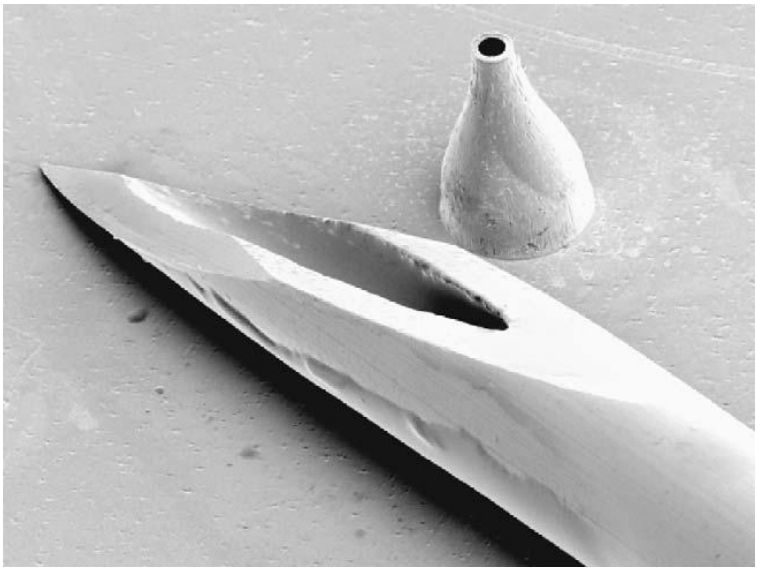

Figure 3: Scanning electron image of a 500 μm tall microneedle next to a 27 gauge hypodermic needle with a diameter of 3.4 mm (Davis et al).

Additionally, by treating the injured area post-injection, the central nervous system may be able to successfully regenerate and heal itself. The gliotic response occurs by recruiting reactive astrocytes to the site of the wound. These astrocytes help to successfully protect and seal the wound as an immediate response, but ultimately inhibit CNS regeneration. Upon arrival at the damaged site, astrocytes release chondroitin and keratan sulphate proteoglycans (types of proteins). These specific proteoglycans have been found to inhibit axonal regeneration and remyelination.[15, 16] Therefore, by combining chondroitin and keratin sulphate inhibitors with the drug to be delivered, CNS regeneration could potentially be avoided. However, further research will need to be performed to ensure that inhibition of these proteoglycans will not have adverse effects on other physiological responses. Injection into the CNS will affect the area of injection,

but will also be absorbed into the blood stream and distributed through the body. Any effect downstream from the site of injection could have hazardous effects on the patient, so additional effects of these inhibitors must be analyzed before use.

Current use of Microneedles

The idea of a micro-sized needle has already been researched extensively. These microneedles have been fabricated from silicon, metals, and polymers. There are unique advantages to microneedles compared to currently used needles. An advantage of using these microneedles is that with a smaller needle comes less compression on the tissue as the needle is inserted. This decreased compression can lead to less compression on pain receptors as well as discomfort associated with the insertion of a large diameter needle.[1] One concern with microneedles is the force needed to break the tissue barrier. By definition, stress is inversely proportional to the area over which a force is applied. Therefore, as the radii of the needle decreases, less force is required to insert the needle.[1] One study, similar to the proposed nanosyringe, used 200 μm long silicon needles with diameters of 40μm.[17] Using these parameters, they were able to successfully break the epidermal skin barrier and inject the desired fluid. In looking at this application, another study showed that fluid flow through MWCNTs with diameters of 7 nm was possible with about 1 atm applied pressure.[18]

Although fluid flow through single walled CNTs (SWCNTs) and multi walled CNTs (MWCNTs) has been demonstrated,[18] flow through vertically aligned CNTs (VACNTs) is still unclear. By combining different sized and shaped CNT arrays with different sized and shaped delivery pores, it is possible to show that fluid flow through VACNTs is possible and efficient.

Lessons Learned

It has been shown that CNTs possess mechanical properties which should allow them to successfully penetrate tissue barriers. Additionally, since fluid flow has been demonstrated through individual CNTs, the idea of demonstrating fluid flow through VACNTs seems probable. Since these VACNTs will be grown at diameters larger than those of individual CNTs, fluid should be able to flow through at applicable rates. Microneedles have already been tested for use as drug delivery systems into delicate tissue to avoid glial scarring. By creating these microneedles out of CNTs, smaller

needle diameters can be achieved and glial scarring can be avoided even more. Finally, although the biocompatibility of CNTs is still unclear, further testing can be performed to better understand this concept. If a CNT based needle could be used and extracted from the tissue without breaking off inside the tissue, then the asbestos-like shape of CNTs would have no adverse affect on the body. Furthermore, through proper purification techniques during CNT fabrication, harmful metals and toxic chemical residues can be removed from the CNT-based microneedles.

The goal of this project is to demonstrate that CNT-based microneedles can be successfully fabricated. To properly function as desired, these microneedles must possess the mechanical strength of raw CNTs while also maintaining their small micrometer diameters. Furthermore, these CNT microneedles must be able to deliver fluid through the CNT to efficiently meet drug delivery purposes. Multiple steps are necessary to fabricate the desired CNT-based microneedle. The two primary steps for this process are pore generation through a silicon wafer, followed by VACNT growth around the pores. The following sections will describe these steps in detail.

CHAPTER 2

EXPERIMENTAL METHODS

Sample Fabriacation

VACNTs were grown on a silicon wafer around a through via in the wafer (Figures 4 and 5). Shapes to be grown and tested included squares, stars, diamonds, triangles, and circles ranging in size from 20 μm to 100μm in width. In total, a maximum of 21 different sample combinations of pore and array variations could be tested from a fully completed wafer. Each sample contained a 10x10 array of homogeneous combinations. These different combinations were achieved using a specifically designed pattern. The photolithographic mask (referred to as Holey-Wafer Mask (HWM), seen in Figure 13) was used to create both the pores and VACNT arrays. The first step, creating the pores through the wafer, was accomplished using the mask in its normal orientation. Once pores were created, the mask was able to be rotated either 90° clockwise (CW), 90°counter-clockwise (CCW), or 180° CW / CCW. This allowed for different shape and size combinations to be achieved.

Pores were etched through the silicon wafer using a Surface Technology Systems Inductively Coupled Plasma (STS ICP) tool. Once pores were been created, the same design pattern used for pores will be developed on the wafer but in a rotated position to overlap different shapes and sizes. Using chemical vapor deposition (CVD) equipment, VACNTs will be grown on the new pattern.

A detailed table showing all possible combinations upon rotation is shown in Figure 16. It should be noted that a 90° CW rotation yields 21 usable combinations, and will therefore yield the most usable combinations. Therefore, the masked was to be rotated in this direction to generate the most samples.

Actual steps to create the final product are shown in detail in Figures 14 and 15 in the appendix. Figure 14 details the steps and tools necessary to create the pores in the wafer, while Figure 15 explains the process required to create the VACNT arrays on top of these pores.

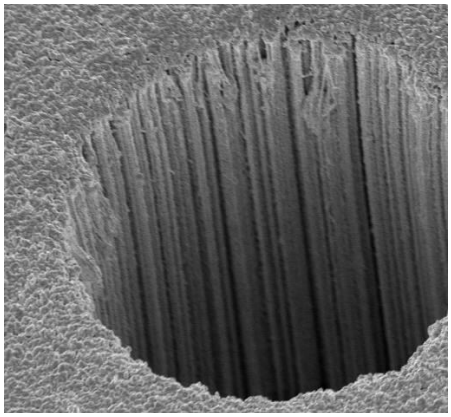

Figure 4: A scanning electron image of VACNTs grown around a circular pore. This image shows the inner ring of the VACNT array.

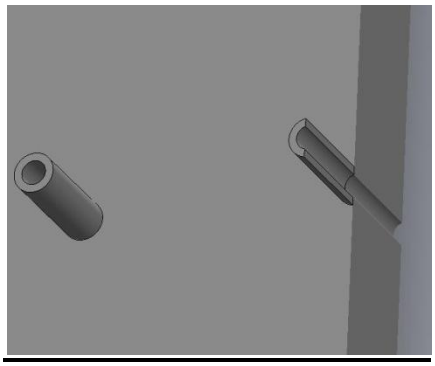

Figure 5: A CAD image of a proposed nanosyringe demonstrates a cross sectional view of the expected results. A tower of VACNTs is shown grown around a circular pore here.

CHAPTER 3

RESULTS

Although no complete sample was fabricated during this project, the total process for creating the samples was critiqued and improved. Multiple attempts were made to create a functional sample but failed at some step in the process. The causes for these failures were documented and taken into account for the following trials. The majority of this project looked at finalizing the process steps necessary to complete the first phase of the experiment, pore generation.

Initially, samples were fabricated on a 3 inch Silicon wafer. In total, five samples were created and developed up to the point of etching. Photoresist application and development parameters and exposure settings were all varied to determine the best setting. Parameter specifics for these samples can be found in the appendix in Figure 17. After the samples had been created, one sample was chosen to be etched. The 3 inch wafer to be etched was mounted onto a 4 inch carrier wafer to protect the machine during the etching process. The wafer was mounted using and placed on top of the carrier wafer, photoresist side up. An error occurred inside the STS ICP during the etching process. Since the 3 inch sample wafer did not fully cover the 4 inch carrier wafer, this left the outer silicon portion of the carrier wafer exposed to the plasma etching. Therefore, the ICP etched away at the sample wafer as well as the carrier wafer edge, causing the carrier wafer to break and shatter during processing. The sample was lost and actions were taken to fix this problem.

Following the failure of the 3 inch wafers, it was noted that 4 inch wafers had to be used in order to utilize the STS ICP. Due to the larger wafer size, photoresist parameters were altered to ensure good results. These parameters can be found in the appendix in Figure 18. After etching in the ICP, the sample was visually analyzed to determine results from the etch process. It could be seen that all pores were not etched completely through the wafer. A cross-sectional analysis was performed to determine the clarity of the pores (Figure 7). This analysis revealed that the pores were being accurately etched with clean side-wall profiles, but not completely through the wafer. Images of the top and back side of the wafer, seen in Figure 6, show that the etch was not complete.

Additionally, visual analysis of the shape clarity showed that the clarity of the shapes was not as definitive as desired (Figures 8 and 9). These results indicated that a longer etch time and alterations to pattern development were necessary.

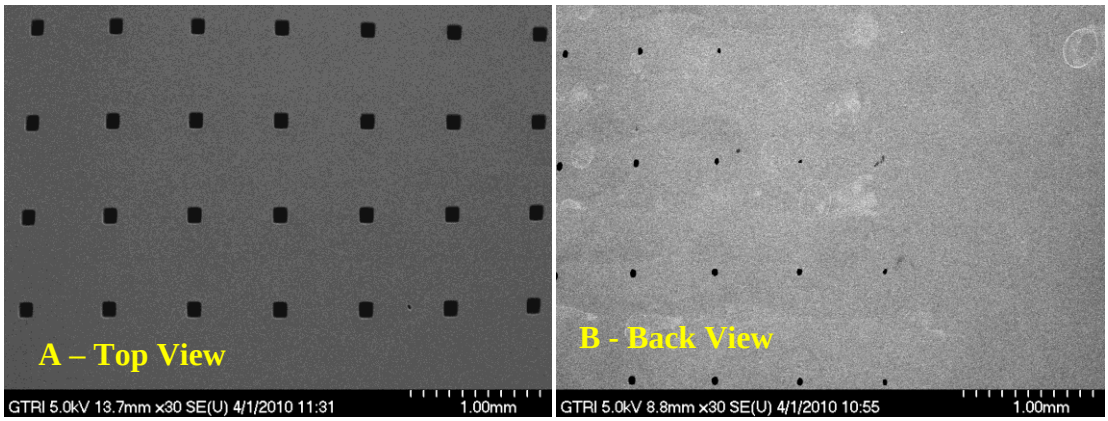

Figure 6: SEM images of top and back side of etched wafer. These images show a 100 μm wide square array. As seen in 6A, the all pores on top are etched. However, in 6B, it can be seen that all pores are not fully etched, with some not even breaking the back side of the wafer.

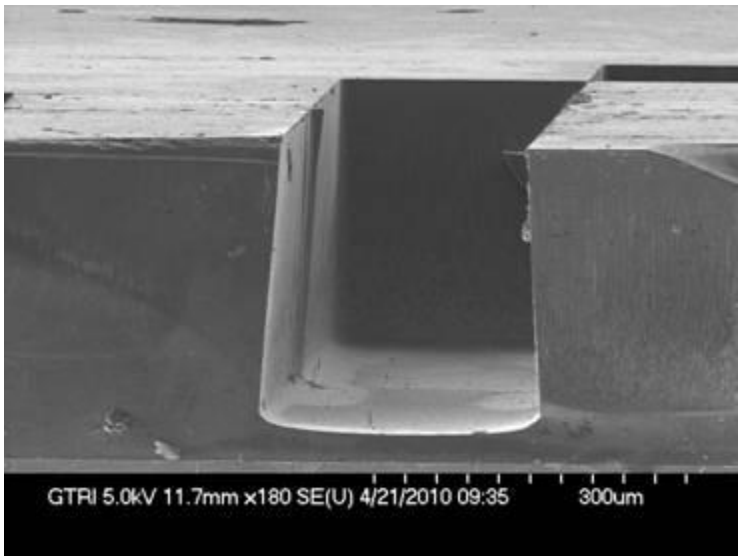

Figure 7: Cross-sectional view of a square pore. It can be seen that the pore has clean side walls and good clarity at the top. However, the etch did not successfully penetrate through the entire wafer.

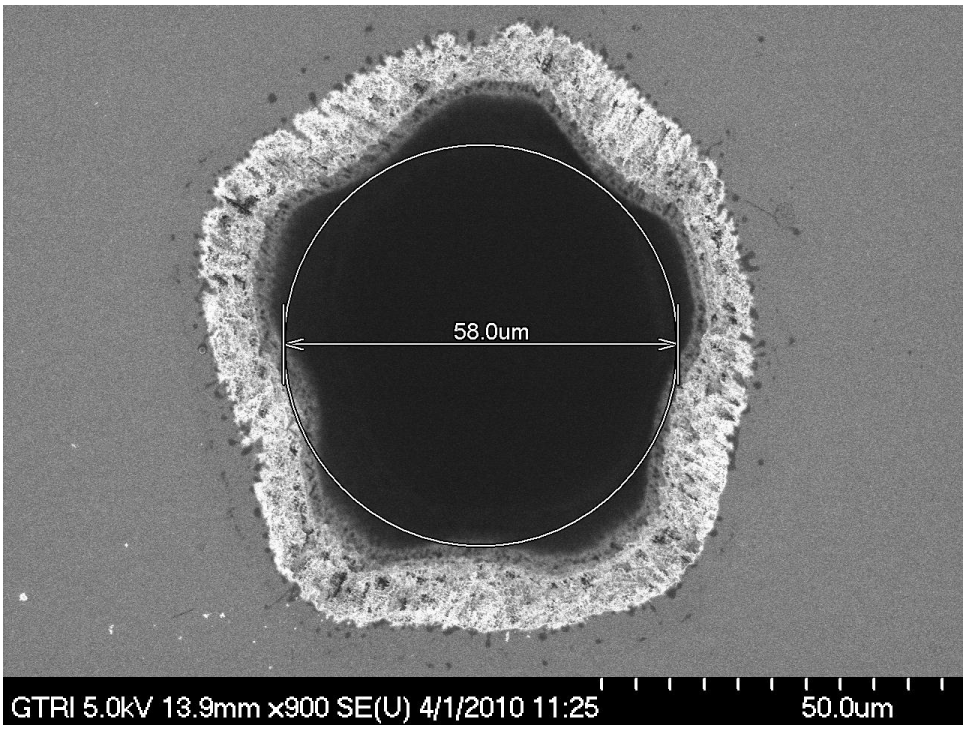

Figure 8: SEM image of a 60 μm wide star. It can be noted that there is poor clarity in the feature definitions with rounded corners and a barely visible star shape.

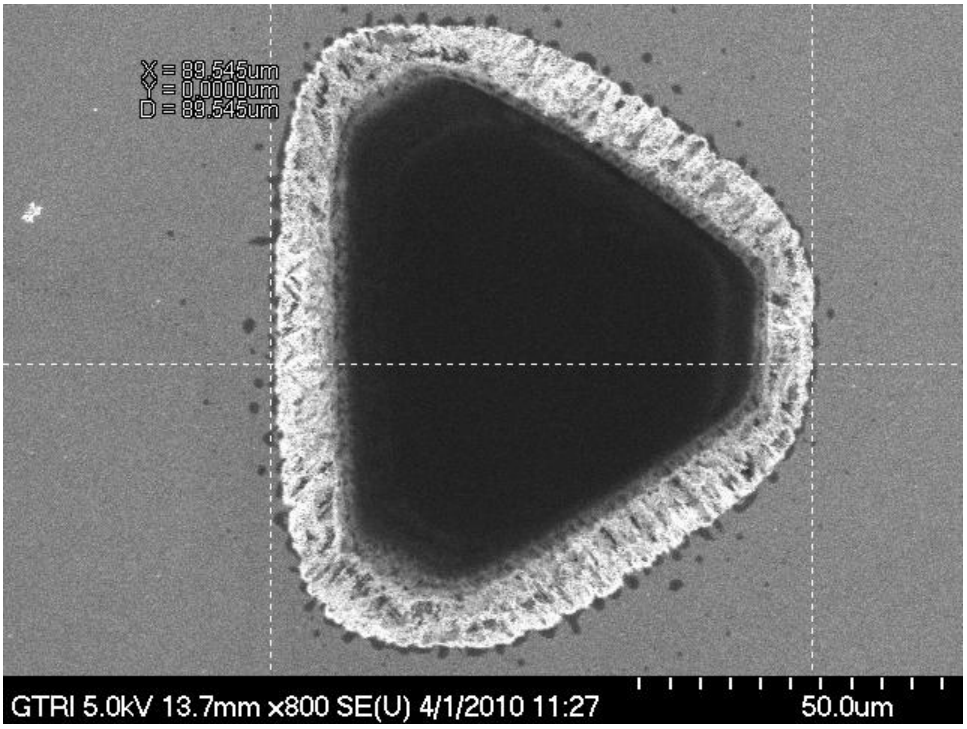

Figure 9: SEM image of a 100 μm wide triangle. It can be seen that the clarity of the larger shapes is better than that of smaller ones. However, the corners of the triangle are still more rounded than desired.

In addition to conducting trials on etching, one trial was performed to analyze potential CNT growth. This trial was performed without pores through the wafers. It was conducted to ensure the pattern generated on the samples would yield viable VACNT arrays. Out of all possible shapes and sizes, the 20 μm square and 60 μm star arrays were grown and visually analyzed. Both samples yielded mixed results, with some shapes growing with good clarity and others with poor shape definition. Therefore, not all shapes were successfully grown. Figures 10 and 11 present samples of successful and failed growth patterns for the 20 μm square array and 60 μm star array. The vertical alignment of the CNTs was also analyzed and determined to be successful from the growth parameters (Figure 12).

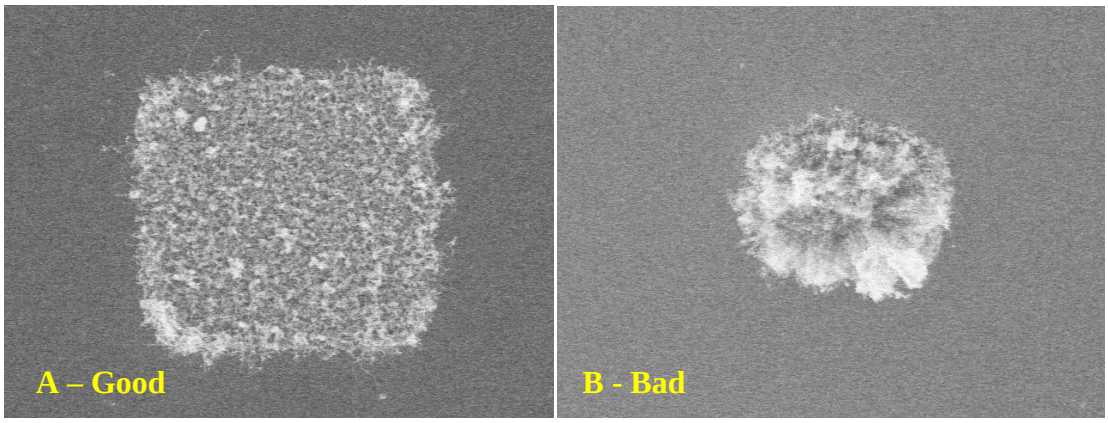

Figure 10: Images of a good and bad 20 μm square sample.

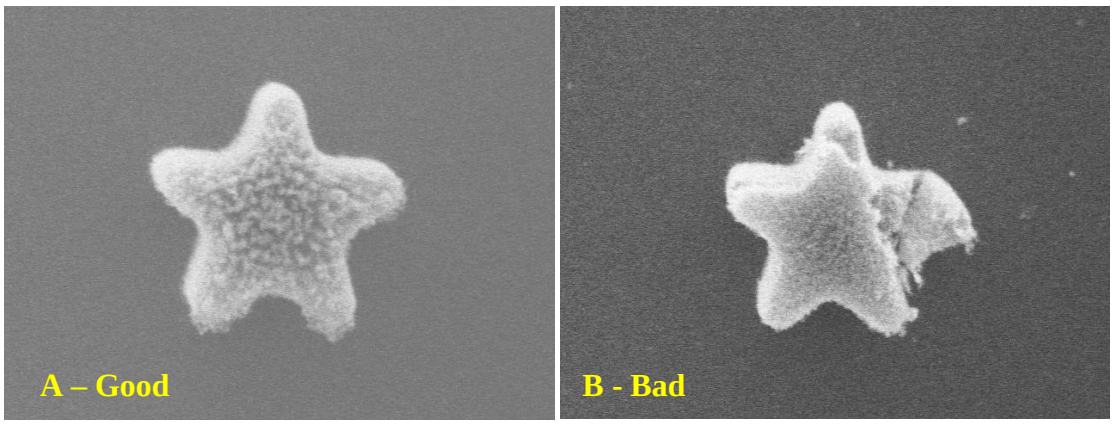

Figure 11: Images of a good and bad 60 μm star sample.

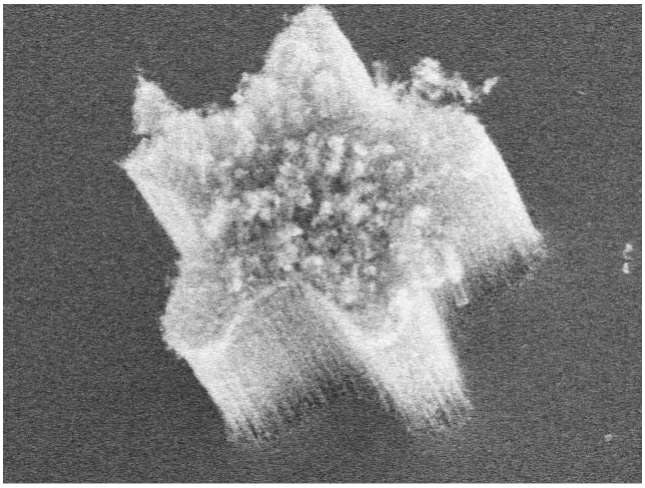

Figure 12: SEM image of the side view of a 60 μm star. It can be seen that there is a clear vertical CNT alignment as desired.

CHAPTER 4

DISCUSSION

Although no complete samples were successfully fabricated, valuable information was gained in regards to the process steps. It was quickly realized that the initially proposed parameters did not perform as desired and needed to be altered. The main areas of improvement came in the areas of photolithography development and through-wafer etching.

Photolithography

After processing multiple samples through the photolithography stages, a better understanding of appropriate parameter settings was determined. Processing the initial samples yielded acceptable results with photoresist deposition and development. Spin times and settings for photoresist application can still be improved and should be investigated further. Initially, spin time and ramp speed for photoresist application were started low and slowly increased until an optimal photoresist spread was achieved. It was determined that a spin speed of 3000 rpm, with a ramp of 1500 rpm/sec for 40 seconds yielded appropriate results. Additionally, a clear decision was never made as to the best type of contact mode during exposure between the wafer and mask. A hard contact was used for these samples, but other types of contact should be analyzed. Furthermore, development time after exposure was never fully determined. Many different development times were tested and yielded positive results. It was determined that the wafer should be developed for 60 seconds initially and then microscopically verified. From here, the wafer should be developed for an additional 15 seconds and verified after each development. Development times varied by a small bit between all samples, demonstrating that development should be performed and microscopically verified before any further steps are taken.

Wafer Etching

Although only two samples were able to etched, each sample provided valuable information for future samples. The first three inch wafer sample shattered in the ICP due to an error with the carrier wafer. It was noted that the exposed silicon on the carrier wafer was etched along with the sample pores, causing the carrier wafer to shatter and

break. This mistake was easily fixed and new samples were fabricated with the four inch wafers. Although the second sample was not fully etched through, it still provided valuable information about the processing. The wafer was diced and visually analyzed to determine the clarity and quality of the results. Cross-sectional analysis showed that the pores were being etched properly and that the etch time had to be increased in order to etch through the wafer. This cross-sectional analysis also demonstrated that an etch phase of 8 seconds followed by a 10 second passivation phase was sufficient. When determining etch time, the main difficulty arose from the varying shapes and sizes. Not all shapes would etch at the same rate or manner. It was known that the larger shapes would etch faster than their smaller counterparts. Additionally, a simple shape such as a circle or square would etch faster than a star due to the complex turns and curves of a star. Etch times were started at 3 hours for fear of damaging the machine. This sample yielded insufficient etching and the etch time was increased for the next trial. Therefore, further studies need to be performed to determine an optimal etching time. From these results, it is believed than an etch time of four hours should be an effective etch time. This optimal time will allow enough time to successfully etch through all smaller and more difficult shapes while still maintaining clarity in the larger ones. It was feared that some shapes may be overexposed to the etching and lose their clarity.

Future Studies

Results from these experiments provided insight into potential uses of VACNT arrays. Future studies should be performed to determine more accurate and precise processing parameters to yield successful results for all trials. Once a successful VACNT array has been grown around pores, these samples can be tested for potential uses. A potential use for these arrays would be for drug delivery into delicate tissues. In order to determine this, a fluid flow analysis would need to be performed to ensure that drug delivery is possible. Additionally, the VACNT arrays can be functionalized to attach specific biochemicals and drugs to them for treatment. Finally, for future use with drug delivery, further testing must be performed on CNT biocompatibility and tissue penetration.

CHAPTER 5
CONCLUSION

This project aimed at developing a process to create a drug eluting nanoelectrode array. Results from this experiment have indicated that a functional VACNT array is possible to create. Trials were performed to better understand the optimal processing parameters required to etch through the wafer and to then grow VACNTs around the pores. All experimental results have been analyzed and taken into account for future trials. It was demonstrated that clear etching results are possible and can be obtained by increasing the etching time. Additionally, results showed that the CNTs can be grown in the desired shapes with acceptable clarity. Therefore, future studies will look at combining all information obtained from these trials and implementing them to create a successful VACNT array.

APPENDIX A: ADDITIONAL FIGURES

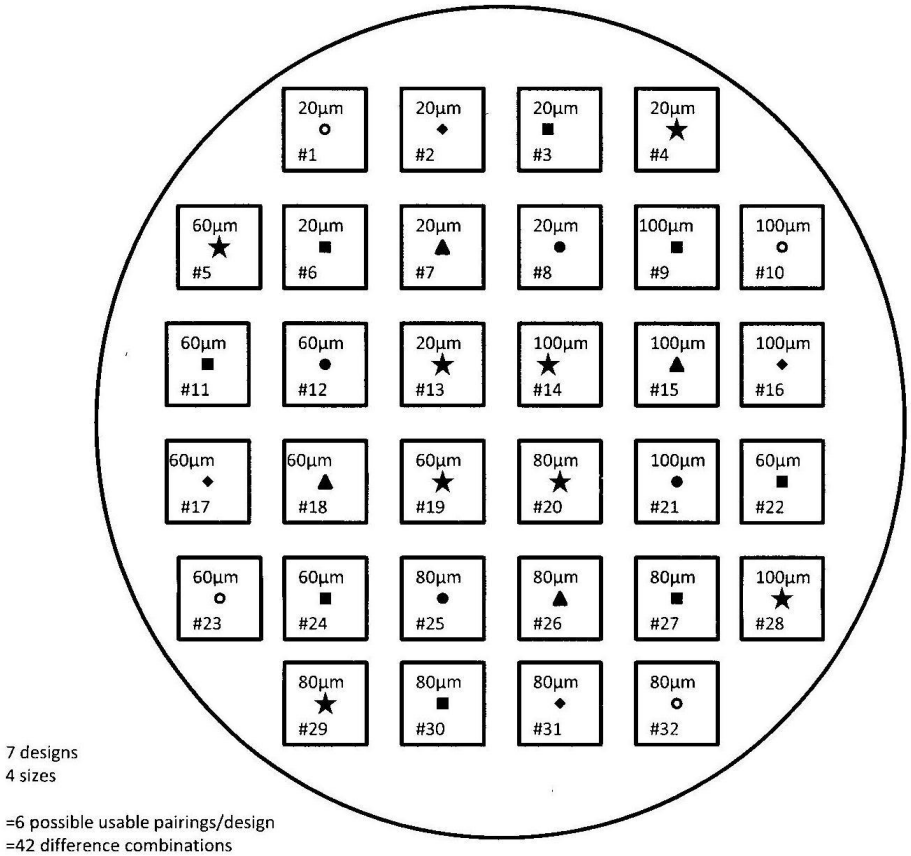

Figure 13: Holey-Wafer Mask. As mentioned previously, 32 different shape and size combinations exist, with each combination consisting of a homogenous 10x10 array of each shape.

Pore Generation

Process	Equipment	Description / Equipment Specifics
Stop-Etch Layer	Unaxis PECVD	Deposit 2 μm thick SiO_2 to back side of wafer
Photoresist(PR) Application	Karl Suss RC8 Spinner	Using Futurrex NR5-8000 Negative PR, apply ~10 μm thick layer.
Soft Bake PR	Hot Plate / Oven	Temperature and time variant.
Exposure	Karl Suss MA-6 Mask Aligner	Hard contact at 365 nm.
Develop	Lab Glassware	Develop using Futurrex RD6 Developer
Hard Bake PR	Hot Plate / Oven	Temperature and time variant.
Mount on Carrier Wafer	Hot Plate & Cool Grease	Heat carrier wafer on 65°C Hot Plate, apply cool grease and mount test wafer on top.
Etch Pores	STS ICP	Optimal time and parameters to be determined.
Strip and Clean Wafer	PR Stripper & CMOS Station	Acetone, Futurrex RR4 PR Stripper, DI Rinse, CMOS Cleaning Station.
Verify Results	Scanning Electron Microscope (SEM)	Hitachi S-800 SEM to verify clarity of pores.

Figure 14: Detailed steps required to create pores through test wafer.

VACNT Array Growth

Process	Equipment	Description / Equipment Specifics
PR Application	CEE 100CB Spinner, Futurrex NR5-8000	Futurrex NR5-8000 PR thickness less than before, thickness TBD.
Soft Bake PR	Hot Plate / Oven	TBD based on thickness.
Exposure	Karl Suss MA-6 Mask Aligner	Hard contact at 365 nm.
Develop	Lab Glassware, Futurrex RD6 Developer	Exposure time by PR thickness.
Hard Bake PR	Hot Plate / Oven	TBD by PR thickness.
Iron Deposit	Thermal Evaporator	0.01 grams of 99.999% pure Fe wrapped around tungsten filament.
Strip and Clean Wafer	PR Stripper & CMOS Station	Acetone, Futurrex RR4 PR Stripper, DI Rinse, CMOS Piranha bath.
Grow CNTs	PECVD or CVD	Recipe TBD
Verify Results	Scanning Electron Microscope (SEM)	Hitachi S-800 SEM to verify successful VACNT array growth

Figure 15: Detailed steps necessary to grow VACNT arrays.

Block #	90° CCW		90° CW		180° CW / CCW	
	Hole	Outside	Hole	Outside	Hole	Outside
1	20 ring	100 ring	20 ring	60 ring	20 ring	80 ring
2	20 diamond	100 diamond	20 diamond	60 diamond	20 diamond	80 diamond
3	20 square	60 square	20 square	60 square	20 square	80 square
4	20 star	100 star	20 star	60 star	20 star	80 star
5	60 star	20 star	60 star	80 star	60 star	100 star
6	20 square	100 square	20 square	60 square	20 square	80 square
7	20 triangle	100 triangle	20 triangle	60 triangle	20 triangle	80 triangle
8	20 circle	100 circle	20 circle	100 circle	20 circle	80 circle
9	100 square	80 square	100 square	20 square	100 square	60 square
10	100 ring	80 ring	100 ring	20 ring	100 ring	60 ring
11	60 square	20 square	60 square	80 square	60 square	60 square
12	60 circle	20 circle	60 circle	80 circle	60 circle	100 circle
13	20 star	100 star	20 star	60 star	20 star	80 star
14	100 star	80 star	100 star	20 star	100 star	60 star
15	100 triangle	80 triangle	100 triangle	20 triangle	100 triangle	60 triangle
16	100 diamond	80 diamond	100 diamond	20 diamond	100 diamond	60 diamond
17	60 diamond	20 diamond	60 diamond	80 diamond	60 diamond	100 diamond
18	60 triangle	20 triangle	60 triangle	80 triangle	60 triangle	100 triangle
19	60 star	20 star	60 star	80 star	60 star	100 star
20	80 star	60 star	80 star	100 star	80 star	20 star
21	100 circle	80 circle	100 circle	20 circle	100 circle	60 circle
22	60 square	80 square	60 square	20 square	60 square	60 square
23	60 ring	20 ring	60 ring	80 ring	60 ring	100 ring
24	60 square	20 square	60 square	20 square	60 square	100 square
25	80 circle	60 circle	80 circle	100 circle	80 circle	20 circle
26	80 triangle	60 triangle	80 triangle	100 triangle	80 triangle	20 triangle
27	80 square	60 square	80 square	100 square	80 square	20 square
28	100 star	80 star	100 star	20 star	100 star	60 star
29	80 star	60 star	80 star	100 star	80 star	20 star
30	80 square	60 square	80 square	60 square	80 square	20 square
31	80 diamond	60 diamond	80 diamond	60 diamond	80 diamond	20 diamond
32	80 ring	60 ring	80 ring	100 ring	80 ring	20 ring

Key	Color	Description
		Usable combination at 90° CCW
		Usable combination at 90° CW
		Usable combination at 180°
		Unusable combination

Figure 16: Table showing possible combinations of pore and array upon different rotations.

Parameter	Value / Setting
PR Spinner	Speed = 2000 rpm, Ramp = 1000 rpm/sec, Time = 40 secs.
Soft Bake	4 mins @ 150 °C
Expose	Contact = Hard Contact, Time = 44 secs @ 365 nm, I = 5.6 mW/cm^2.
Hard Bake	3.5 mins @ 100 °C
Develop	105 secs
Etch	Etch = 10 secs, Pass = 8 secs, 750 cycles

Figure 17: Trial 1 parameters for samples created using 3 inch wafers. This sample broke during the etching process.

Parameter	Value / Setting
PR Spinner	Speed = 3000 rpm, Ramp = 1500 rpm/sec, Time = 40 secs.
Soft Bake	3.5 mins @ 150 °C
Expose	Contact = Hard Contact, Time = 31 secs @ 365 nm, I = 6.0 mW/cm^2.
Hard Bake	3.5 mins @ 100 °C
Develop	90 secs
Etch	Etch = 10 secs, Pass = 8 secs, 750 cycles

Figure 18: Trial 2 parameters using 4 inch wafers. This sample did not etch completely through the wafer for all arrays.

REFERENCES

1. *Zahn JD AD, A.P. Pisano, D. Liepmann. Continuous On-Chip Micropumping for Microneedle Enhanced Drug Delivery. Biomedical Microdevices. 19 July 2009 2004;6(3):183-190.*

2. *Edwards SL JSC, J.A. Werkmesiter, J.A.M Ramshaw. Tubular micro-scale multiwalled carbon nanotube-based scaffolds for tissue engineering. Biomaterials. 2009;30:1725-1731.*

3. *Zheng LX, O'Connell MJ, Doorn SK, et al. Ultralong single-wall carbon nanotubes. Nat Mater. 2004;3(10):673-676.*

4. *Sinha N JY. Carbon Nanotubes for Biomedical Applications. IEEE Transactions on Nanobioscience. 2005;4(2):180-195.*

5. *Foldvari M BM. Carbon nanotubes as functional excipients for nanomedicines: I. pharmaceutical properties. Nanomedicine: Nanotechnology, Biology, and Medicine. 2008;4:173-182.*

6. *Harrison BS AA. Carbon nanotube applications for tissue engineering. Biomaterials. 2007;28:344-353.*

7. *Watari F NT, A. Yokoyama, M. Uo, T. Akasaka, Y. Sato, S. Abe, Y. Totsuka, K. Tohji. Material nanosizing effect on living organisms: non-specific, biointeractive, physical size effects. J. R. Soc. Interface. 2009;6:371-388.*

8. *Foldvari M MB. Carbon nanotubes as functional excipients for nanomedicines: II. Drug delivery and biocompatibility issues. Nanomedicine: Nanotechnology, Biology, and Medicine. 2008;4:183-200.*

9. *Xu F JX, J. Ji, J. Shen. A novel biomimetric polymer as amphiphilic surfactant for soluble and biocompatible carbon nanotubes (CNTs). Colloids and Surfaces B: Biointerfaces. 2008;67:67-72.*

10. *Cheng J CMC, L.M. Veca, W.L. Poon, P.K. Chan, L. Qu, Y. Sun, S.H. Cheng. Acute and long-term effects after single loading of functionalized multi-walled carbon nanotubes into zebrafish (Danio rerio). Toxicology and Applied Pharmacology. 2009;235:216-225.*

11. *Rolls A SR, Schwartz M. The bright side of the glial scar in CNS repair. Nature Reviews Neuroscience. July 19, 2009 2009;10(March 2009):235-241.*

12. *Rasouli NB, P. Dinh, K. Cahill, S. Suryadevara, R. Gupta. Resection of Glial Scar following Spinal Cord Injury. Journal of Orthopaedic Research. 2008(July 2009):931-936.*

13. *Rorvik D. Catalog/Handbook of Fine Chemicals- Syringe Needle Dimensions. 1994-1995; http://academic.evergreen.edu/projects/biophysics/technotes/fabric/syringe.htm.*

14. *Davis SP, Landis BJ, Adams ZH, Allen MG, Prausnitz MR. Insertion of microneedles into skin: measurement and prediction of insertion force and needle fracture force. Journal of Biomechanics. 2004;37(8):1155-1163.*

15. *Silver J, Miller JH. Regeneration beyond the glial scar. Nature Reviews. Neuroscience. 2004;5(2):146-156.*

16. *McKeon R, Schreiber R, Rudge J, Silver J. Reduction of neurite outgrowth in a model of glial scarring following CNS injury is correlated with the expression of*

inhibitory molecules on reactive astrocytes. J. Neurosci. November 1, 1991 1991;11(11):3398-3411.

17. *Häfeli U, Mokhtari A, Liepmann D, Stoeber B. In Vivo Evaluation of a Microneedle-Based Miniature Syringe for Intradermal Drug Delivery. Biomedical Microdevices. In Press.*

18. *Majumder M CM, Andrews R, Hinds BJ. Nanoscale hydrodynamics: enhanced flow in carbon nanotubes. Nature. 2005;438:44.*